

University of San Diego

Digital USD

Chemistry and Biochemistry: Faculty
Scholarship

Department of Chemistry and Biochemistry

1-6-2022

Radical-Initiated Brown Carbon Formation in Sunlit Carbonyl–Amine–Ammonium Sulfate Mixtures and Aqueous Aerosol Particles

Natalie G. Jimenez
University of San Diego


Kyle D. Sharp
University of San Diego


Tobin Gramyk
University of San Diego

Duncan Z. Ugland
University of San Diego

Matthew-Khoa Tran
University of San Diego

Follow this and additional works at: https://digital.sandiego.edu/chemistry_facpub

 See next page for additional authors

 Part of the [Chemistry Commons](#)

Digital USD Citation

Jimenez, Natalie G.; Sharp, Kyle D.; Gramyk, Tobin; Ugland, Duncan Z.; Tran, Matthew-Khoa; Rojas, Antonio; Rafla, Michael A.; Stewart, Devoun; Galloway, Melissa M.; Lin, Peng; Laskin, Alexander; Cazaunau, Mathieu; Pangu, Edouard; Doussin, Jean-François; and De Haan, David O., "Radical-Initiated Brown Carbon Formation in Sunlit Carbonyl–Amine–Ammonium Sulfate Mixtures and Aqueous Aerosol Particles" (2022). *Chemistry and Biochemistry: Faculty Scholarship*. 41.
https://digital.sandiego.edu/chemistry_facpub/41

This Article is brought to you for free and open access by the Department of Chemistry and Biochemistry at Digital USD. It has been accepted for inclusion in Chemistry and Biochemistry: Faculty Scholarship by an authorized administrator of Digital USD. For more information, please contact digital@sandiego.edu.

Radical-Initiated Brown Carbon Formation in Sunlit Carbonyl–Amine–Ammonium Sulfate Mixtures and Aqueous Aerosol Particles

Abstract

Brown carbon (BrC) formed from glyoxal+ammonium sulfate (AS) and methylglyoxal+AS reactions photobleaches quickly, leading to the assumption that BrC formed overnight by Maillard reactions will be rapidly destroyed at sunrise. Here, we tested this assumption by reacting glyoxal, methylglyoxal, glycolaldehyde, or hydroxyacetone in aqueous mixtures with reduced nitrogen species at pH 4–5 in the dark and in sunlight (>350 nm) for at least 10 h. The absorption of fresh carbonyl+AS mixtures decreased when exposed to sunlight, and no BrC formed, as expected from previous work. However, the addition of amines (either methylamine or glycine) allowed BrC to form in sunlight at comparable rates as in the dark. Hydroxyacetone+amine+AS aqueous mixtures generally browned faster in sunlight than in the dark, especially in the presence of HOOH, indicating a radical-initiated BrC formation mechanism is involved. In experiments with airborne aqueous aerosol containing AS, methylamine, and glyoxal or methylglyoxal, browning was further enhanced, especially in sunlight (>300 nm), forming aerosol with optical properties similar to “very weak” atmospheric BrC. Liquid chromatography-electrospray ionization-mass spectrometry (LC-ESI-MS) analysis of aerosol filter extracts indicates that exposure of methylglyoxal+AS aqueous aerosol to methylamine gas, sunlight, and cloud processing increases incorporation of ammonia, methylamine, and photolytic species (e.g., acetyl radicals) into conjugated oligomer products. These results suggest that when amines are present, photolysis of first-generation, “dark reaction” BrC (imines and imidazoles) initiates faster, radical-initiated browning processes that may successfully compete with photobleaching, are enhanced in aqueous aerosol particles relative to bulk liquid solutions, and can produce BrC consistent with atmospheric observations.

Keywords

secondary brown carbon, photosensitization, photobrowning, aqueous SOA, oligomerization, aldehydes

Disciplines

Chemistry

Notes

Final published version available at <https://doi.org/10.1021/acsearthspacechem.1c00395>

Author(s)

Natalie G. Jimenez, Kyle D. Sharp, Tobin Gramyk, Duncan Z. Uglund, Matthew-Khoa Tran, Antonio Rojas, Michael A. Rafla, Devoun Stewart, Melissa M. Galloway, Peng Lin, Alexander Laskin, Mathieu Cazaunau, Edouard Pangui, Jean-François Doussin, and David O. De Haan

1 Radical-initiated brown carbon formation in sunlit
2 carbonyl – amine – ammonium sulfate mixtures and
3 aqueous aerosol particles

4 *Natalie G. Jimenez,¹ Kyle D. Sharp,¹ Tobin Gramyk,¹ Duncan Z. Uglund,¹ Matthew-Khoa Tran,¹*
5 *Antonio Rojas,¹ Michael A. Rafla,¹ Devoun Stewart,^{1††} Melissa M. Galloway,^{1†} Peng Lin,²*
6 *Alexander Laskin,² Mathieu Cazaunau,³ Edouard Pangui,³ Jean-François Doussin,³ David O.*
7 *De Haan,^{1*}*

8
9 1: Department of Chemistry and Biochemistry, University of San Diego, 5998 Alcalá Park, San
10 Diego CA 92117 USA

11 2: Environmental Molecular Sciences Laboratory, Pacific Northwest National Laboratory,
12 Richland, Washington 99352, USA, now at Department of Chemistry, Purdue University, West
13 Lafayette IN 47907 USA

14 3: Laboratoire Interuniversitaire des Systèmes Atmosphériques (LISA), UMR7583, CNRS,
15 Université Paris-Est Créteil (UPEC) et Université de Paris, Institut Pierre Simon Laplace (IPSL),
16 Créteil, France

17 †: now at Department of Chemistry, Lafayette College, Easton PA 18042 USA

18 ††: now at Department of Chemistry, Sacramento City College, 3835 Freeport Blvd.
19 Sacramento, CA 95822 USA

20

21 * Corresponding author: ddehaan@sandiego.edu, (619) 260-6882, (619) 260-2211 fax

22 ABSTRACT: Brown carbon (BrC) formed from glyoxal+ammonium sulfate (AS) and
23 methylglyoxal+AS reactions photobleaches quickly, leading to the assumption that BrC formed
24 overnight by Maillard reactions will be rapidly destroyed at sunrise. Here we tested this
25 assumption by reacting glyoxal, methylglyoxal, glycolaldehyde or hydroxyacetone in aqueous
26 mixtures with reduced nitrogen species at pH 4-5 in the dark and in sunlight (>350 nm) for at least
27 10 h. The absorbance of fresh carbonyl+AS mixtures decreased when exposed to sunlight, and no
28 BrC formed, as expected from previous work. However, the addition of amines (either
29 methylamine or glycine) allowed BrC to form in sunlight at comparable rates as in the dark.
30 Hydroxyacetone+amine+AS aqueous mixtures generally browned faster in sunlight than in the
31 dark, especially in the presence of HOOH, indicating a radical-initiated BrC formation mechanism
32 is involved. In experiments with airborne aqueous aerosol containing AS, methylamine, and
33 glyoxal or methylglyoxal, browning was further enhanced, especially in sunlight (>300 nm),
34 forming aerosol with optical properties similar to “very weak” atmospheric BrC. LC-ESI-MS
35 analysis of aerosol filter extracts indicates that exposure of methylglyoxal+AS aqueous aerosol to
36 methylamine gas, sunlight, and cloud processing increases incorporation of ammonia,
37 methylamine, and photolytic species (*e.g.* acetyl radicals) into conjugated oligomer products.
38 These results suggest that when amines are present, photolysis of 1st-generation, “dark reaction”
39 BrC (imines and imidazoles) initiates faster, radical-initiated browning processes that may
40 successfully compete with photobleaching, are enhanced in aqueous aerosol particles relative to
41 bulk liquid solutions, and can produce BrC consistent with atmospheric observations.

42 **Introduction**

43 Aerosol particles negatively impact human health,¹⁻⁸ and aerosol particles that absorb light,
44 such as brown carbon (BrC), also exacerbate climate change.⁹⁻¹⁸ Determining ways to limit
45 atmospheric BrC concentrations is desirable on both accounts. While a majority of brown carbon
46 is emitted directly from incomplete combustion (primary BrC), about a third is formed in the
47 atmosphere via poorly-characterized reactions in the gas or aqueous phase.^{19, 20} Significant
48 amounts of secondary BrC are thought to be formed by aqueous Maillard reactions involving
49 closed-shell reactions of small, water-soluble carbonyl species with ammonium or amine salts,²¹⁻
50 ²⁷ producing imine intermediates²⁸ which oligomerize to form light-absorbing species (the “imine
51 pathway”),²⁹⁻³³ and by aqueous photo-oxidation of phenolic species,³⁴⁻⁴⁰ especially when catalyzed
52 by Fe(III) ions.⁴¹⁻⁴³ Co-oxidation of glyoxal and dissolved SO₂ has also been recently shown to
53 form BrC.⁴⁴ The relative importance of these various BrC formation pathways in the atmosphere
54 has not been determined.

55 BrC in the atmosphere is subject to aging processes which are even less understood than BrC
56 formation.⁴⁵⁻⁵¹ Light-absorbing molecules may be destroyed by hydroxyl radicals or other oxidant
57 species that diffuse into the aqueous phase or are formed in situ.⁴⁸ Photobleaching of BrC may
58 also occur, triggered by direct light absorption^{27, 43, 45} or indirectly via reaction with
59 “photosensitizer” species.⁵²⁻⁵⁴ Rapid photobleaching of BrC formed in mixtures of glyoxal or
60 methylglyoxal with AS has been observed in several studies performed in bulk-phase solution.⁵⁵⁻
61 ⁵⁹ In some more complex systems, photolysis, photooxidation, or oxidation by radical species can
62 at least temporarily increase BrC formation,^{54, 57, 60, 61} especially in evaporating droplets.³² In the
63 vast majority of these studies, BrC is formed in the dark, then photolyzed or photooxidized
64 separately, simulating a diurnal cycle, guided by an implicit assumption that BrC forms at night

65 and is destroyed during the day. This two-step experimental design, however, does not address
66 the extent to which BrC might form in the sunlit atmosphere, perhaps aided by radical-initiated
67 reactions. Experimental photobleaching results are also dependent on photolysis wavelengths,
68 highlighting the importance of simulating the solar spectrum in laboratory simulations of
69 photobleaching.

70 In this work, we study the effects of sunlight and an OH radical source (hydrogen peroxide,
71 HOOH) on aqueous-phase BrC formation involving reactions of glyoxal (GX), methylglyoxal
72 (MG), hydroxyacetone (HA), and glycolaldehyde (GAld) with ammonium sulfate, glycine, and
73 methylamine in order to determine whether daytime radical-initiated mechanisms play a
74 significant role.

75

76 **Methods**

77 Bulk-phase studies. The initial UV/vis absorption spectra of bulk phase aqueous reaction
78 mixtures (0.25 M of each reactant, pH set to 4 with oxalic or sulfuric acid) were recorded with 2
79 nm spectral resolution over the range 200-800 nm using 1 cm quartz cuvettes in a diode array
80 absorption spectrometer (HP8452A). Each reaction mixture was then placed in a capped Pyrex
81 vial with a 50% transmittance cutoff of ~350 nm, and the set of vials were exposed to ambient
82 midday sunlight for 4 h (~12-4 pm on days with little or no cloud coverage in San Diego,
83 California, day-to-day solar intensity varied by ~30%). A matching set of solutions were placed
84 in most experiments at the same location under aluminum foil so that they would react in the dark
85 at comparable temperatures. Temperature monitoring of select vials indicated that dark and sunlit
86 samples remained within 3 °C of each other, unless specified otherwise. After the 4-h reaction
87 time, the UV/vis spectra of the contents of each vial were recorded and the samples were stored in

88 the dark at 4 °C until the next day. The process was repeated for at least two subsequent days for
89 each vial. Minimal spectral changes were observed during overnight cold storage. The initially
90 measured absorbance spectrum for each mixture was subtracted from subsequently measured
91 spectra to generate ΔAbs difference spectra, to show the change in absorbance during sample aging.
92 Absorbance changes were converted to mass absorption coefficients changes (ΔMAC) by the
93 following equation:

$$94 \quad \Delta MAC = \frac{\ln(10) \Delta Abs}{b C_{org}}$$

95 where b is the pathlength in cm and C_{org} is the sum of the concentrations of the carbonyl reactant
96 species and the amine species (if any) in the reaction mixture in g cm^{-3} . The Angstrom absorbance
97 exponents (AAE) were also characterized by power law fits to absorbance spectra in the range 330
98 – 400 nm. This fit range was adjusted to longer wavelengths by up to 50 nm when necessary to
99 avoid saturated absorbance readings ($Abs > 2.0$).

100 Aerosol studies. Mixtures of carbonyls, AS, and amines (0.056 M of each reactant) were
101 aspirated into a 300 L Tedlar chamber. The airborne aerosol particles were then aged for 1 h in
102 midday ambient sunlight, or indoors away from sunlight in control experiments. After 1 h of
103 aging, aerosol particles were collected onto Teflon filters, which were then extracted in 10 mL
104 deionized water (>18 M Ω). The absorbance of filter extracts was analyzed by diode array
105 absorption spectroscopy (HP8452A) in 1 cm cuvettes. ΔMAC values were calculated using C_{org}
106 calculated from the mass increase of the filter during sampling divided by the extraction volume;
107 AAE fits were determined as described above.

108 Simulation chamber experiment / high-resolution MS analysis. 100 mM MG and 10 mM AS /
109 30 mM MG solutions were atomized (TSI 3076) and, for control experiments, 100 μg of diffusion-

110 dried aerosol was immediately collected onto teflon filters (Tisch, 1.0 μm pore size) without any
111 chamber exposure time. The same AS+MG mixture was also atomized without diffusion drying
112 into the humidified, 4.2 m^3 CESAM chamber, which has been described earlier.^{62, 63} There, these
113 deliquesced seed particles were exposed to 2 ppm methylamine gas, 80 minutes of simulated
114 sunlight, and 1-2 cloud events of 5 to 10 min. duration each, triggered by a combination of water
115 vapor injection and a gradual, 10% pressure reduction to reach supersaturation. Chamber
116 experimental conditions are summarized in Table S1. After processing in the chamber concluded,
117 aerosol were collected onto Teflon filters at a flow of 15 L/min over 16 h, while chamber pressure
118 was held constant with a compensating flow of dry nitrogen, resulting in a continuous reduction
119 in RH during sampling. All filters were kept frozen at -20C until extraction by acetonitrile and
120 analysis using a HPLC/PDA/HRMS platform.⁶⁴ The instrument consists of a Surveyor Plus
121 system (including HPLC pump, autosampler and PDA detector), a standard IonMAX electrospray
122 ionization (ESI) source, and a high resolution LTQ-Orbitrap mass spectrometer (all modules are
123 from Thermo Electron, Inc.). Details about the experimental setup, data acquisition, peak
124 deconvolution, and molecular formula assignment have been described previously.³¹ Exact masses
125 detected for peaks with areas greater than 10^6 and elevated relative to blank extract runs are
126 reported here.

127

128 **Results and Discussion**

129 Carbonyl + AS mixtures. Changes in absorbance (expressed as ΔMAC) of aqueous mixtures
130 containing 0.25 M carbonyl compounds and 0.25 M AS reacting for 10-14 h are shown in Figure
131 1. (See Figure S1 for corresponding ΔAbs graph.) Under dark conditions (green lines), the relative
132 levels of browning observed, $\text{MG} \gg \text{GX} > \text{GAld} \sim \text{HA}$, matches previous observations.⁶⁵ In fact,

133 MAC increases at wavelengths below 400 nm in MG+AS and GX+AS mixtures after 6 h are quite
134 similar to those reported after 4 days at the same pH and concentrations,⁶⁵ indicating that UV-
135 absorbing reaction products form in these mixtures in hours rather than days under these
136 conditions. In HA+AS and GAlD+AS mixtures, however, significant browning is not observed at
137 any wavelength even after 14 h of reaction time. Figure 1 shows that MAC increases in the visible
138 range (> 400 nm) remains negligible (< 5 cm² g⁻¹) in all samples through 14 h of reaction time.
139 Visible browning – the development of an absorbance “tail” extending to wavelengths beyond 400
140 nm – is quite slow in acidified bulk aqueous samples, developing only after a few days of reaction
141 time.^{23, 25, 65}

142 The effects of sunlight on duplicate reaction mixtures are shown in Figure 1 (gold lines). During
143 the initial 2 h of photolysis, the overall absorbance of the GX+AS and MG+AS samples declined.
144 Clearly, no BrC is forming in sunlight, validating the conclusion of other studies that BrC formed
145 overnight by dark GX+AS and MG+AS reactions would be rapidly destroyed during the day.^{57, 58}
146 Indeed, BrC formed by dark GX+AS and MG+AS reactions has been shown to photobleach
147 rapidly, with a lifetime on the order of minutes,⁵⁵⁻⁵⁸ much faster than its slow formation over hours
148 in bulk samples, even at slightly elevated temperatures here. For GX and MG, MAC declines in
149 sunlight in Figure 1 are strongest at wavelengths where the most browning occurred in the dark,
150 producing Δ MAC spectra that look like negative mirror images of those recorded under dark
151 conditions. Declining absorbance observed in sunlight indicates a loss of reactants (or loss of
152 rapidly-formed products already present in the initial $t = 0$ absorbance measurement) due to direct
153 photolysis or reactions with photosensitizers.

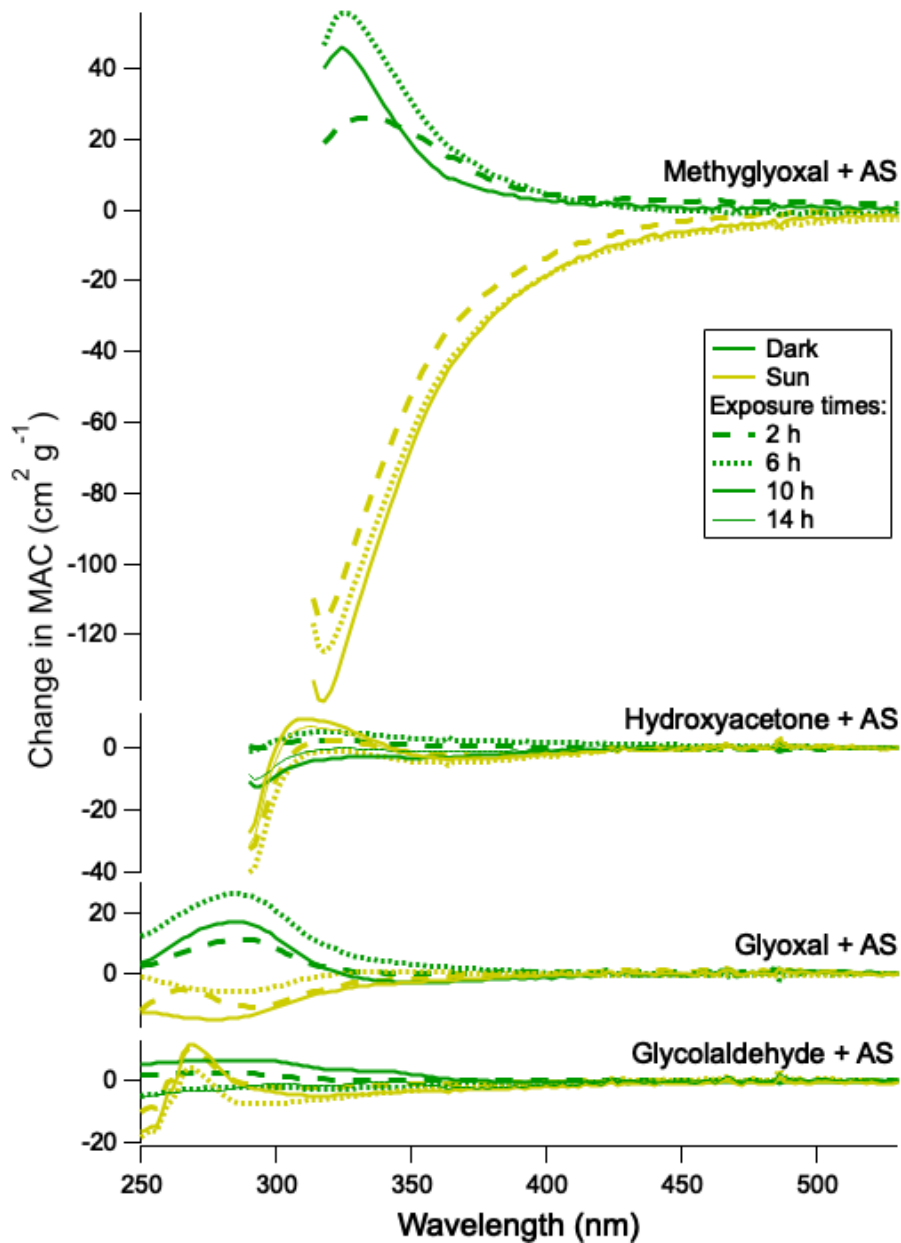


Figure 1: Changes in wavelength-dependent mass absorption coefficients (MAC) of aqueous reaction mixtures containing 0.25 M carbonyl compound and 0.25 M ammonium sulfate after varying times of dark reaction at 21-28 °C (green lines) or reaction in sunlight at 23-35 °C (gold lines). All data is shown on equivalent vertical scale; gaps in data

171 indicate off-scale

172 absorbance readings, such that *MAC* changes cannot be calculated accurately. Reaction times are
 173 indicated by line type: 2h (dashed line), 6h (dotted line), 10h (thick solid line), and 14h (thin line,
 174 GAld and HA only). Color indicates sunlit (gold) or dark (green) conditions).

175

176 For GAlD+AS and HA+AS reaction mixtures (which did not brown significantly during 14 h
177 in the dark), the effects of sunlight are subtle and wavelength-dependent. Sunlight caused the
178 absorbance of the GAlD+AS sample to decrease at most wavelengths, but also caused an
179 absorbance band centered at 270 nm to appear. Similarly, sunlight caused an absorbance band at
180 312 nm to increase in the HA+AS sample. Each of these bands increased in height by only ≤ 12
181 $\text{cm}^2 \text{g}^{-1}$ (+0.08 absorbance units) during 10 h. In contrast, absorbance did not increase at any
182 wavelength in sunlit MG+AS and GX+AS mixtures.

183 Carbonyl + amine + AS mixtures. It is sometimes suggested that the rapid photobleaching of
184 MG+AS and GX+AS mixtures can be generalized to all imine-based brown carbon systems. The
185 validity of this inference was tested in experiments where carbonyl compounds reacted with
186 AS+glycine and AS+methylamine mixtures (Figures 2, S2, and S3).

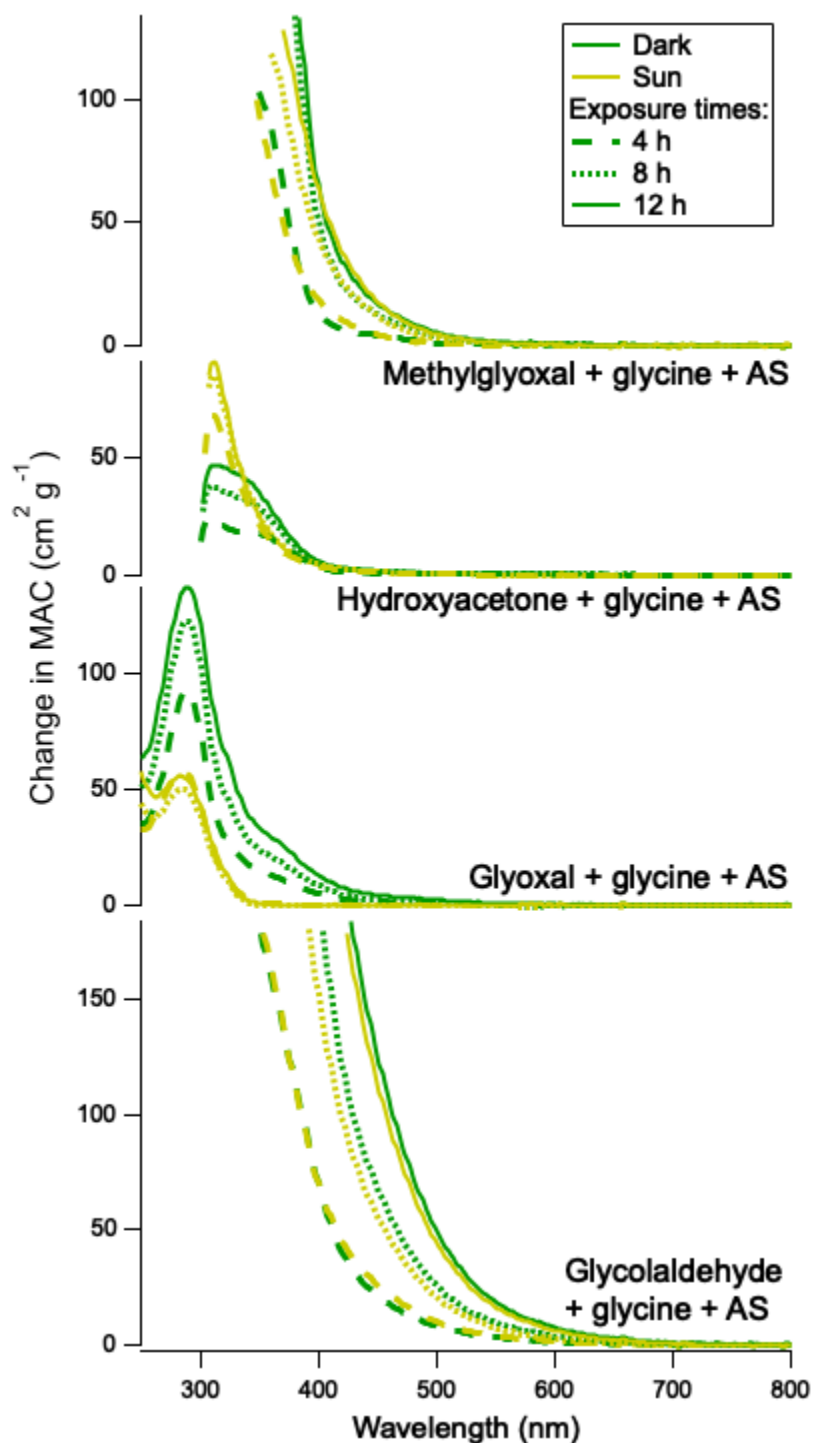


Figure 2: Changes in wavelength-dependent mass absorption coefficients of paired aqueous reaction mixtures containing 0.25 M carbonyl compound, 0.25 M ammonium sulfate, and 0.25 M glycine after varying reaction times in sunlight (gold lines) or dark conditions (green lines). Each sun/dark sample pair was temperature-matched to within 3 °C throughout reaction, except MG, where temperatures diverged by up to 8 °C. All data is shown on equivalent vertical scale; traces that do not extend to 250 nm indicate off-scale absorbance readings, such that ΔMAC

208 cannot be calculated accurately. Reaction times indicated by line type: 4 h (dashed), 8 h (thick

209 dotted), 12 h (solid). Color indicates sunlit (gold) or dark (green) conditions). See Figure S2 for
210 corresponding ΔAbs graphs.

211 The addition of an amine to the mixtures profoundly changes their browning behavior in the
212 dark and especially in the sun, even though pH is held constant. In the dark, UV absorbance is
213 intensified by amine addition in all four reaction mixtures, as observed in previous studies.^{65, 66}
214 Absorbance clearly extends into the visible range for GX, MG and GAld+glycine+AS solutions
215 after a few hours reaction time. In sunlight, the presence of glycine counteracts the photobleaching
216 of starting materials that was observed in carbonyl+AS solutions. Instead, absorbance now
217 increases under both dark and sunlit conditions for all carbonyl+glycine+AS solutions. With
218 GX+glycine+AS, the magnitude of the absorbance increase is less in sunlight than in the dark,
219 indicating that photobleaching is occurring but cannot keep pace with BrC production. The same
220 is true with HA+glycine+AS at wavelengths >335 nm. Browning in sunlight and in the dark is
221 nearly identical for MG and GAld+glycine+AS solutions, suggesting that either the BrC products
222 are resistant to photolytic degradation or that rates of photobleaching and an additional
223 photolytically-activated browning process are nearly balanced. Generally similar browning
224 behavior was observed using methylamine rather than glycine as the amine species (Figure S3).
225 Methylamine-containing mixtures browned in sunlight for 12 h, but more slowly than in the dark
226 for MG, GAld (> 340 nm), and GX+methylamine+AS (> 300 nm) reaction mixtures, which
227 suggests that photobleaching is slower than BrC production in these systems.

228 The extreme differences between sunlit browning in carbonyl+amine+AS mixtures and rapid
229 photobleaching in carbonyl+AS mixtures demonstrate that the effects of sunlight on BrC formation
230 and photobleaching cannot be generalized across imine-based BrC reaction systems. These bulk-

231 phase experiments show that carbonyls can form BrC even in the daytime atmosphere if they are
232 present with amines in aqueous aerosol particles at high enough concentrations.

233 In contrast to the three aldehydes tested, the ketone species HA unexpectedly browned faster in
234 sunlight than in the dark when mixed with AS and an amine species, especially at wavelengths
235 below 350 nm. This indicates the existence of a fast browning mechanism initiated by a radical
236 or photosensitizer species. This “photobrowning” was observed below 350 nm in 5 out of 8
237 replicate experiments on HA+methylamine+AS mixtures (Figure S4) including all three runs
238 where methylamine was acidified with sulfuric acid. In other runs, acidifying to the same pH with
239 oxalic acid unexpectedly⁶⁷ enhanced the dark browning of these mixtures without having a
240 consistent effect on sunlit samples. Within each acidification group (using sulfuric or oxalic acid),
241 while the absorbance that developed in dark HA+methylamine+AS mixtures varied from
242 experiment to experiment, likely due to day-to-day temperature variation, sunlit experiments
243 exhibited a larger variation in absorbance. This higher variation in photobrowning may be caused
244 by the additional variable of solar intensity, and/or by an important role of some photolytically-
245 active species in the mixture, such as a photosensitizer first-generation product or trace oxidant
246 precursor absorbed from the air when the reaction vial is opened. We explore the role of one such
247 oxidant precursor species, hydrogen peroxide, in the next section.

248 Effects of HOOH on BrC formation. Figure 3 summarizes the effects of two different
249 concentrations of HOOH for HA+methylamine+AS mixtures in the dark and in sunlight. In the
250 dark, the addition of HOOH (light and dark blue lines) suppresses the buildup of light-absorbing
251 products, especially at higher HOOH concentrations (dark blue lines), likely due to direct oxidation
252 of BrC species. High concentrations of HOOH initially suppress the accumulation of BrC species
253 in sunlight, too (dark red lines), but after a few hours BrC formation accelerates and eventually

254 overtakes that of HOOH-free samples. Since HOOH is slowly being photolyzed by sunlight and
255 converted to OH radicals, we hypothesize that the initial large excess of HOOH rapidly destroys
256 BrC products as they form, as seen in dark samples, while OH radicals trigger BrC production
257 reactions that are faster than, and distinct from, the dark pathways involving only closed-shell
258 reactants. Thus, it is only when most excess HOOH is used up that radical-initiated brown carbon
259 products can rapidly accumulate. Furthermore, the similarity of absorbance spectra in all sunlit
260 samples after 12 h reaction times is consistent with some baseline level of OH radical production
261 in HOOH-free samples from photosensitization by starting materials or first-generation products.⁶⁸

262 The hypothesis that OH catalyzes rapid brown carbon production in HA+amine+AS mixtures
263 while excess HOOH destroys brown carbon was supported by experiments where the timing and
264 amounts of HOOH added and the amine species were varied. With 10x less initial HOOH added
265 (Figure 3), some suppression of browning was still observed in the dark (light blue lines), but
266 rapid browning in sunlight (orange lines) started immediately, without the initial induction period
267 seen with higher HOOH concentrations. In other experiments, 0.25 M HOOH was added not only
268 at $t = 0$ but also at 4, 8, and 12 h (Figure S6) to test the effects of replenishing excess HOOH. In
269 these experiments, no significant browning was observed, and some photobleaching occurred
270 below 325 nm, further supporting the idea that excess HOOH destroys brown carbon or its
271 precursors.

272 Similar results were observed in experiments where methylamine was replaced with glycine
273 (Figure S7). Although absorbance increased more slowly at 350 nm with glycine, the most brown
274 carbon still formed when solutions containing lower levels (0.025 M) of HOOH were exposed to
275 several hours of sunlight. Clearly sunlight and especially OH radicals enhance BrC production in

276 HA+amine+AS reaction mixtures, pointing to the importance of radical-initiated BrC formation
277 pathways in this reaction system.
278

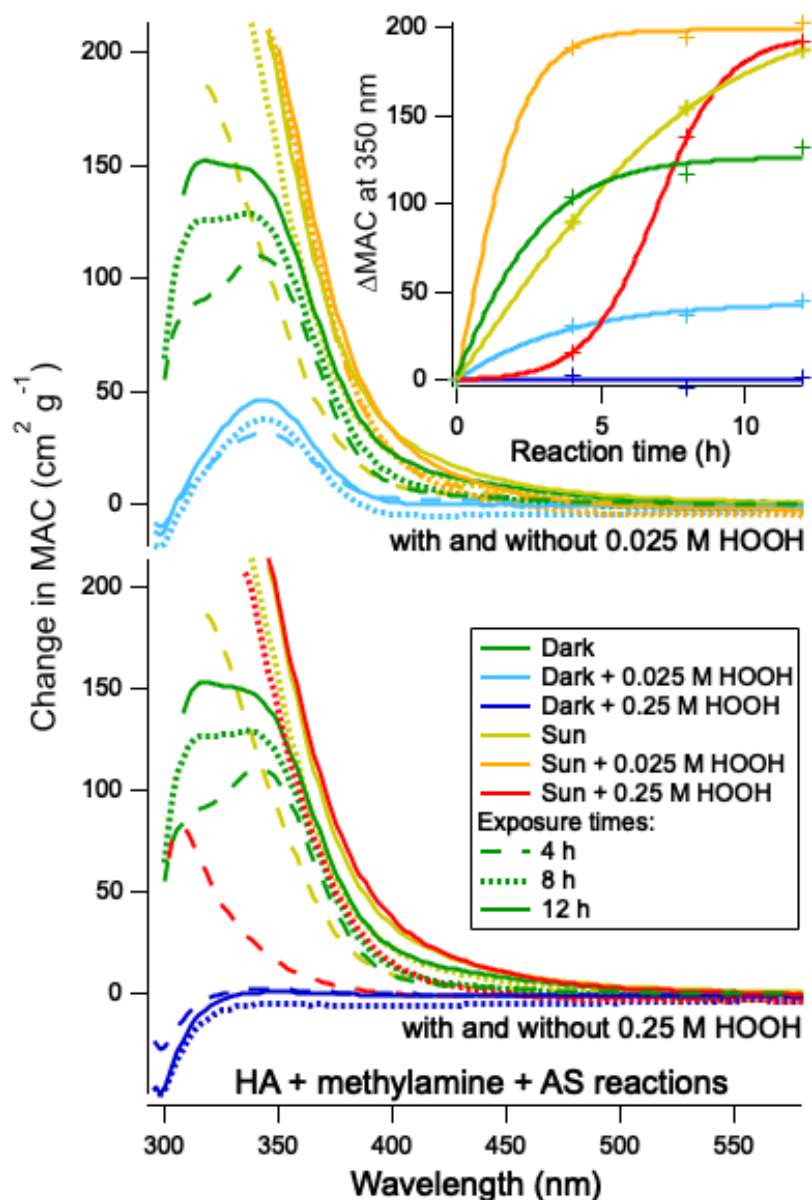


Figure 3: Changes in wavelength-dependent mass absorption coefficients of paired reaction mixtures containing 0.25 M HA, methylamine, and AS in sunlight (gold) or dark (green) after 4 h (dashed lines), 8 h (dotted lines), or 12 h (solid lines). Top panel: comparison with identical mixtures with 0.025 M HOOH in sunlight (orange) or in dark (light blue).

296 Lower panel: comparison with identical mixtures with 0.25 M HOOH in sunlight (red) or in dark
 297 (dark blue). Inset: ΔMAC at 350 nm vs time, using same color code. See Figure S5 for
 298 corresponding ΔAbs graphs.

299

300 Carbonyl + amine + AS aerosol particles. Since absorption spectra⁵⁰ and browning chemistry

301 can differ in suspended aerosol particles from that in bulk solutions,³² aqueous aerosol particles

302 were generated in Tedlar bags and exposed to either in full-spectrum sunlight or ambient indoor
303 light while suspended in air, before filtration and extraction. The mass absorption coefficients
304 (MAC) of filter extracts from suspended aerosol experiments are summarized in Figure 4. For the
305 GX + methylamine + AS system (top panel), aerosol-phase browning between 300 and 400 nm is
306 more pronounced when particles are aged in sunlight rather than indoor ambient light, with or
307 without added HOOH. This is the opposite of what is observed at these wavelengths when bulk
308 solutions are exposed to sunlight (Figure S3, 3rd panel), demonstrating that photolytically-driven
309 radical reactions can produce GX-derived BrC material in sunlight, not just at night, at enhanced
310 rates in suspended aqueous aerosol particles compared to bulk liquid samples. While the addition
311 of 1.7 mM HOOH to the aerosol-generation liquid suppressed BrC formation to some extent in
312 both sunlight and indoor experiments, the 1 h photolysis time in these experiments may have been
313 insufficient to eliminate excess HOOH. In any case, sunlit samples still browned more than dark
314 samples in the presence of HOOH.

315

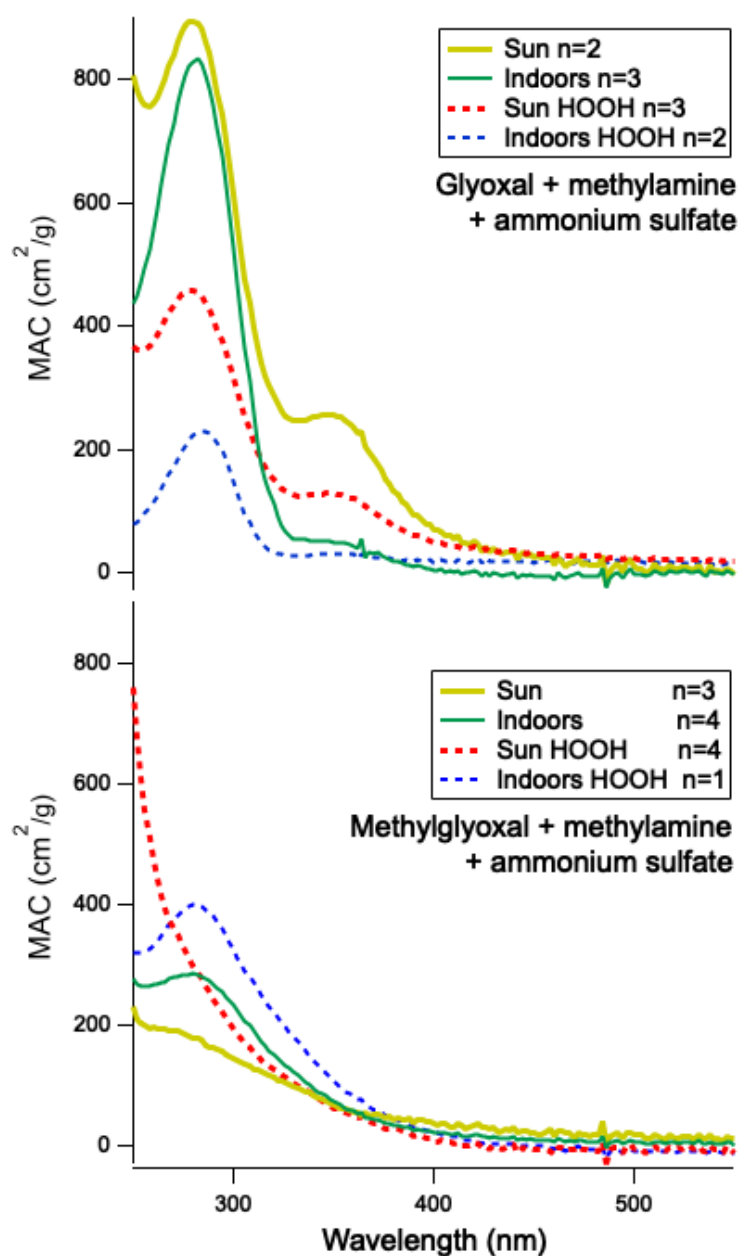


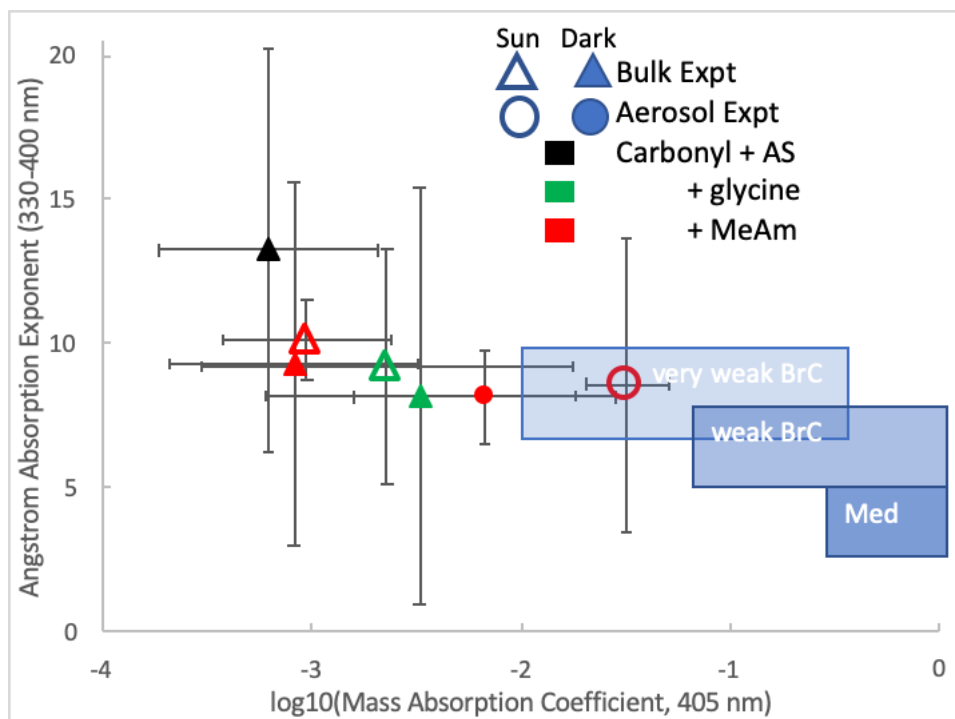
Figure 4: Wavelength-dependent mass absorption coefficients of aerosol filter extracts from small chamber experiments. Aqueous aerosol were generated from solutions containing 0.056 M dicarbonyl compound, methylamine, and AS, aged for ~1 h in sunlight (gold lines) or ambient indoor light (green lines). With added 0.0017 M HOOH in sunlight (red dashes), or ambient indoor light (blue dashes). Top panel: GX. Bottom panel: MG. Numbers of experiments averaged into each line are shown in legends.

333

334 For MG+methylamine+AS aerosol, slightly more browning is observed in particles protected
 335 from sunlight than in those exposed to sunlight (Figure 4 bottom panel), even in the presence of
 336 HOOH, but the difference is smaller than in bulk solutions (Figure S3, 1st panel). Taken together,
 337 these results for dicarbonyl+methylamine+AS solutions suggest that photosensitization / radical-

338 induced browning can be enhanced in aerosol particles relative to bulk liquid solutions with the
339 same reactants present. This is important because most BrC photobleaching studies to date have
340 been performed on bulk liquid solutions,⁵⁵⁻⁵⁹ even if the brown carbon was initially formed in
341 suspended aerosol.⁵⁸

342 The optical parameters of BrC from each experiment are compared to the recent atmospheric
343 BrC classification scheme of Saleh *et al.*^{69, 70} in Figure 5. It can be seen that BrC formed in dark,
344 bulk-phase reactions between carbonyl species and AS (black triangle) does not match
345 atmospheric BrC in absorptivity, expressed as $\log(\text{MAC}_{405})$, and on average has a wavelength
346 dependence (expressed as $\text{AAE}_{330-400}$) that is steeper. (Since no BrC forms from this system in
347 sunlight, this condition cannot appear in Figure 5.) The addition of an amine species to bulk-phase
348 carbonyl-AS mixtures brings the wavelength dependence of absorption into the range of very weak
349 BrC and allows brown carbon to form in the sun, but the average MAC values are still lower than
350 atmospheric BrC. MAC values extracted from aerosol-phase experiments are higher than in bulk-
351 phase experiments, especially in experiments where suspended aerosol were exposed to 1 h of
352 sunlight. Under these sunlit aerosol conditions, the BrC formed from carbonyl+AS+amine
353 reactions, on average, matched the wavelength dependence and absorptivity of the “very weak”
354 class of BrC observed in the atmosphere.



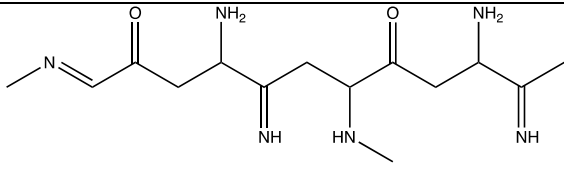
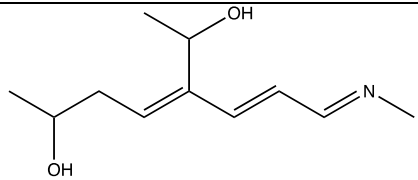
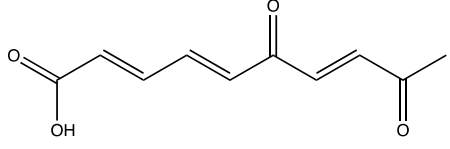
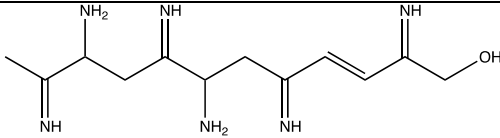
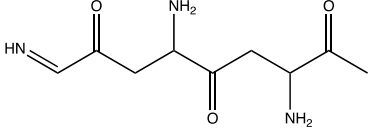
355
 356 Figure 5: Optical parameters of BrC formed in this study compared to Saleh's field-based BrC
 357 classification scheme, graphed as Angstrom absorption exponent vs MAC₄₀₅. Each data point
 358 represents an average of experiments with different carbonyl compounds; shapes indicate bulk
 359 phase (triangle) or aerosol phase (round) experiments, while fill indicates dark (filled) or sunlit
 360 (open symbol) conditions. All experiments contain carbonyl species and ammonium sulfate.
 361 Symbol color indicates amine present: no amine (black), methylamine (red), or glycine (green).

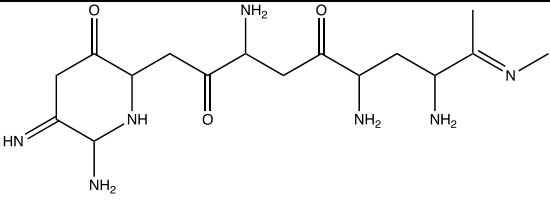
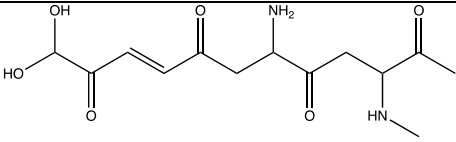
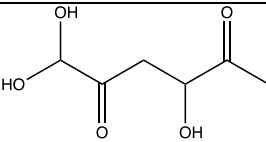
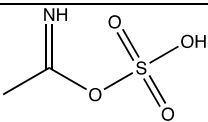
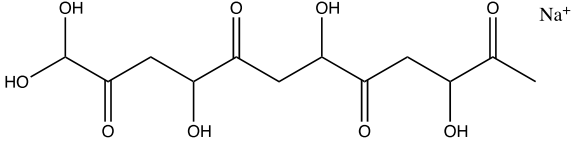
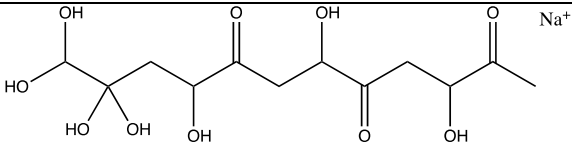
362
 363 Chemical analysis of aerosol particles. Additional MG+methylamine+AS experiments with
 364 offline LC-ESI-MS analysis were conducted in the CESAM chamber to further our mechanistic
 365 understanding of the photolytic browning pathway involving amines. In these experiments we
 366 compared pure MG seed aerosol particles and 3:1 MG:AS seed aerosol particles with no chamber
 367 exposure to 3:1 MG:AS aerosol particles that had been exposed to 2 ppm methylamine gas, 80
 368 minutes of simulated sunlight, and cloud processing in the chamber. A list of observed ions with

369 exact masses, peak area ranking, minimum light/dark experiment peak area ratios, and proposed
 370 molecular formulae, structures, and precursor species is shown in Table 1. Product molecules
 371 detected only with chamber exposure to methylamine and sunlit clouds are labeled “unique,” while
 372 remaining products are listed in order from most increased to most decreased due to chamber
 373 exposure.

374

375 Table 1: Changes in Reaction Products Detected in Methylglyoxal+AS Aerosol Particles Upon
 376 Exposure to Methylamine Gas, Simulated Sunlight, and Cloud Processing

Exptl. ion m/z	Peak area rank, post- exposure	Peak area ratio vs seed particles	Neutral formula (precursor species)	Ionization	Δ^a (ppm)	Proposed structure
311.2191	12	unique ^b	C ₁₄ H ₂₆ N ₆ O ₂ (4MG 2MA 4NH ₃)	H ⁺	1.5	
198.1477	13	unique ^b	C ₁₁ H ₁₉ NO ₂ (5AAld 1MA)	H ⁺	8.4	
217.0500	17	unique ^b	C ₁₀ H ₁₀ O ₄ (3MG 1AAld - 1CO ₂)	Na ⁺	-10.6	
267.1928	19	unique ^b	C ₁₂ H ₂₂ N ₆ O (3MG 1HA 6NH ₃)	H ⁺	1.9	
214.1188	5	3.5	C ₉ H ₁₅ N ₃ O ₃ (3MG 3NH ₃)	H ⁺	1.8	

368.2410	10	2.0	C ₁₆ H ₂₉ N ₇ O ₃ (5MG 1MA 6NH ₃)	H ⁺	0.1	
301.1410	1	1.8	C ₁₃ H ₂₀ N ₂ O ₆ (4MG 1MA 1NH ₃)	H ⁺	-3.5	
185.0420	3	0.038	C ₆ H ₁₀ O ₅ (2MG)	Na ⁺	2.9	
140.0021	4	0.022	C ₂ H ₅ NSO ₄ (1AAld 1SO ₄ 1NH ₃)	H ⁺	-2.4	
329.0843	7	0.012	C ₁₂ H ₁₈ O ₉ (4MG)	Na ⁺	1.6	
347.0950	2	0.0034	C ₁₂ H ₂₀ O ₁₀ (4MG)	Na ⁺	1.1	
126.0391	6	0.0024	C ₂ H ₄ O ₅	NH ₄ ⁺	9.0	Oxalic acid hydrate

377 Seven peaks detected by positive ion mode ESI-MS that increased in sunlight are listed, followed
 378 by the five largest peaks that decreased in sunlight (ratio < 1), listed in order of decreasing light-
 379 to-dark experiment peak area ratios. Molecular formulas were detected as H⁺ adducts unless
 380 otherwise stated. Abbreviations: MG = methylglyoxal. MA = methylamine. NH₃ = ammonia.
 381 AAld = acetaldehyde or acetyl radical. -1CO₂ = photolytic decarboxylation. HA =
 382 hydroxyacetone, formed from MG photolysis. SO₄ = sulfate ion. **a**: nominal – measured mass.
 383 **b**: detected only in experiments with simulated sunlight, listed in order from largest to smallest
 384 peak areas.

385

386 At the bottom of Table 1, it can be seen that major MS peaks that decreased in size after chamber
 387 exposure to methylamine and sunlit clouds (ratios < 1) all have exact masses that match species
 388 containing 0 or 1 nitrogen atom per molecule. These species include methylglyoxal dimer and
 389 tetramer species (likely formed by aldol condensation) and a proposed imine-organosulfate species

390 that was present only in experiments where ammonium sulfate was included in seed particles. On
391 the other hand, peaks that increased in size during chamber exposure (Table 1 top) matched
392 molecular formulae with 2 to 7 N / molecule. Exposure to methylamine in the chamber appears
393 to have increased both methylamine and ammonia incorporation into aqueous-phase products,
394 likely due to methylamine's favorable exchange reaction with dissolved ammonium salts,
395 producing ammonia and methylaminium ions. Calculating an average number of N / molecule
396 weighted by peak area as described in the SI, we find that chamber exposure of methylglyoxal+AS
397 aerosol to methylamine and sunlit clouds increased the number of nitrogens per detected organic
398 molecule from 1.0 to 2.0, dominated by the production of $C_{13}H_{20}N_2O_6$ (m/z 301.1410) and its
399 incorporation of one methylamine and one ammonia molecule.

400 Unique peaks that were seen only after chamber exposure to methylamine and sunlit clouds were
401 assigned to proposed molecular structures containing 3 – 6 double bonds, and appear to form from
402 precursors including methylamine, acetaldehyde / acetyl radicals, and/or HA. The formation of
403 the unique $C_{10}H_{10}O_4$ m/z 217.0500 product also appears to involve oxidation followed by
404 decarboxylation, which can be catalyzed by ammonium salts.⁷¹ Chamber exposure increased the
405 weighted average number of conjugated double bonds per molecule from 1.0 (non-conjugated) to
406 3.0, again dominated by the production of $C_{13}H_{20}N_2O_6$ (m/z 301.1410) with its four double bonds,
407 three of which are conjugated. In summary, exposure to methylamine, sunlight, and cloud
408 processing results in the conversion of MG oligomers into more conjugated product molecules that
409 incorporate more nitrogen (both methylamine and ammonia) and photolysis products (acetyl
410 radicals and HA).

411 While it was apparent in a recent study that acetyl radicals played a central role in the photo-
412 oligomerization chemistry of methylglyoxal,⁶³ the source of these radicals was unclear. Hydration

413 of methylglyoxal, even in the gas phase,⁷² removes any absorbance bands in the actinic range,⁷³
414 suggesting that direct photolysis of aqueous methylglyoxal is unlikely in the atmosphere or in any
415 realistic laboratory simulation. Aqueous solutions of HA, GX, and GAld are less light-absorbing
416 than MG, making direct photolysis of these dissolved compounds even less likely. Once small
417 carbonyl species react with reduced nitrogen compounds in the aqueous phase, however, imines
418 and derivatized N-containing heterocyclic products are formed.⁷⁴ These products are more
419 strongly light absorbing than the reactants, moving absorbance into the actinic range where light
420 absorption can occur.^{23, 25} In dark reactions with GX, common atmospheric amines such as glycine
421 and methylamine have been shown to be more effective than ammonium salts at generating C-N
422 bonds⁶⁶ and light-absorbing products.^{65, 66} Thus, it is likely that photolysis of first-generation
423 carbonyl + amine BrC products generate the radical species that trigger further oligomerization
424 and brown carbon production.

425 For example, imidazole derivatives are a class of photosensitizer C-N reaction products^{52, 75, 76}
426 that have been detected in aqueous-phase reactions of AS with all four carbonyl compounds used
427 in this study.⁷⁴ Replacing ammonia with primary amines in the dark chemical mechanism
428 produces a permanently charged imidazolium ring whose absorbance is red-shifted by ~10 nm
429 compared to a neutral imidazole ring formed with ammonia.⁷⁷ Additional functional groups
430 attached to the carbon atoms in heterocyclic rings further red-shift the absorbance bands.⁷⁴ The
431 increased overlap of such N-containing reaction products with the solar spectrum is expected to
432 increase production of radicals and excited-state photosensitizer species in the aqueous aerosol
433 phase. In recent AS-free studies of BrC aerosol formation by methylglyoxal+methylamine
434 reactions,⁶³ it was noted that imidazolium derivatives were formed upon exposure to methylamine
435 gas, but then were greatly reduced or eliminated upon exposure to sunlight, suggesting that such

436 compounds are the source of not only triplet carbon excited state species but also photolysis
437 fragment radicals that trigger further oligomerization and browning in sunlight. This result is
438 consistent with the MS product analysis in Table 1, where N-methyl imidazole species were not
439 detected in aerosol after combined methylamine and sunlight exposure in the chamber.

440 Radical and/or excited state species, once produced, will rapidly react with nearby molecules in
441 crowded aqueous environments, and especially at the air-water interface where surface-active
442 molecules accumulate.⁷⁸ This effect has been noted in bulk aqueous-phase experiments on
443 carbonyl compounds, where oxidation by OH radicals generated oligomeric products only at high
444 concentrations due to accretion reactions between organic radical intermediates and other organic
445 molecules.^{79, 80} A similar effect is evidently at work in the light-activated formation of brown
446 carbon oligomers in the carbonyl+AS+amine aqueous reaction system. Moreover, the dominance
447 of light-activated radical reaction pathways involving surface-active BrC may be explain the
448 observed divergent behavior between photobleaching experiments performed in bulk solution and
449 in suspended droplets.⁵⁰

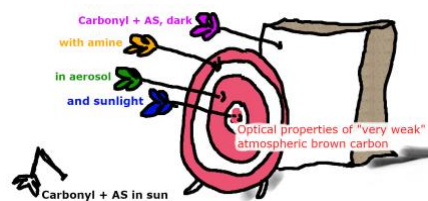
450

451 **Acknowledgments.** This work was funded by NSF grants AGS-1523178 and AGS-1826593.
452 The CESAM chamber aerosol aging experiments were part of a project that has received funding
453 from the European Union's Horizon 2020 research and innovation program under grant
454 agreement No 730997. CNRS-INSU is gratefully acknowledged for supporting CESAM as an
455 open facility through the National Instrument label, as well as the AERIS data center
456 (<https://www.aeris-data.fr/>) for hosting, curating, and distributing CESAM chamber data via
457 EUROCHAMP-2020 databases. The HPLCPDA-ESI-HRMS measurements were performed at
458 the Environmental Molecular Sciences Laboratory (EMSL), a national scientific user facility

459 located at PNNL, and sponsored by the Office of Biological and Environmental Research of the
460 U.S. DOE.

461 **Supplemental Information:** Description of calculations of peak-weighted N atoms and
462 conjugated double bonds per detected molecule, additional absorption change graphs,
463 MG/GX/GAld/HA+methylamine+AS experiment data, effects of acidifying samples with oxalic
464 vs sulfuric acid, data summaries of additional HOOH addition experiments, and summary table of
465 large chamber aerosol processing experiments.

466 **TOC artwork**



467

468 **References**

- 469 1. Schwartz, J., Air pollution and daily mortality: a review and meta analysis. *Environ. Res.*
470 **1994**, *64*, (1), 36-52. doi:10.1006/enrs.1994.1005
- 471 2. Schwartz, J., What are people dying of on high air pollution days? *Environmental Research*
472 **1994**, *64*, (1), 26-35. doi:10.1006/enrs.1994.1004
- 473 3. Kao, A. S.; Friedlander, S. K., Temporal variations of particulate air pollution: a marker for
474 free radical dosage and adverse health effects? *Inhal. Toxicol.* **1995**, *7*, (1), 149-156.
475 doi:10.3109/08958379509014278
- 476 4. Gilmour, P. S.; Brown, D. M.; Lindsay, T. G.; Beswick, P. H.; MacNee, W.; Donaldson, K.,
477 Adverse health effects of PM10 particles: involvement of iron in generation of hydroxyl
478 radical. *Occup Environ Med* **1996**, *53*, (12), 817-822. doi:10.1136/oem.53.12.817
- 479 5. Harrison, R. M.; Yin, J., Particulate matter in the atmosphere: which particle properties are
480 important for its effects on health? *The Science of The Total Environment* **2000**, *249*, (1-3), 85-
481 101. doi:10.1016/s0048-9697(99)00513-6
- 482 6. Poschl, U., Atmospheric aerosols: Composition, transformation, climate and health effects.
483 *Angew Chem Int Edit* **2005**, *44*, (46), 7520-7540. doi:DOI 10.1002/anie.200501122
- 484 7. Kennedy, I. M., The health effects of combustion-generated aerosols. *Proceedings of the*
485 *Combustion Institute* **2007**, *31*, (2), 2757-2770.
486 doi:<https://doi.org/10.1016/j.proci.2006.08.116>
- 487 8. Wu, S.; Deng, F.; Wei, H.; Huang, J.; Wang, X.; Hao, Y.; Zheng, C.; Qin, Y.; Lv, H.; Shima,
488 M.; Guo, X., Association of cardiopulmonary health effects with source-appointed ambient
489 fine particulate in Beijing, China: A combined analysis from the Healthy Volunteer Natural
490 Relocation (HVNR) study. *Environ Sci Technol* **2014**, *48*, (6), 3438-3448.
491 doi:10.1021/es404778w
- 492 9. Ramanathan, V.; Li, F.; Ramana, M. V.; Praveen, P. S.; Kim, D.; Corrigan, C. E.; Nguyen, H.;
493 Stone, E. A.; Schauer, J. J.; Carmichael, G. R.; Adhikary, B.; Yoon, S. C., Atmospheric brown
494 clouds: hemispherical and regional variations in long-range transport, absorption, and
495 radiative forcing. *J. Geophys. Res.* **2007**, *112*, (D12), D22S21/1-D22S21/26.
496 doi:10.1029/2006JD008124
- 497 10. Bahadur, R.; Praveen, P. S.; Xu, Y.; Ramanathan, V., Solar absorption by elemental and brown
498 carbon determine from spectral observations. *Proc. Natl. Acad. Sci. (USA)* **2012**, *109*, (43),
499 17366-17371. doi:10.1073/pnas.1205910109
- 500 11. Feng, Y.; Ramanathan, V.; Kotamarthi, V. R., Brown carbon: a significant atmospheric
501 absorber of solar radiation? *Atmos. Chem. Phys.* **2013**, *13*, (17), 8607-8621. doi:10.5194/acp-
502 13-8607-2013
- 503 12. Laskin, A.; Laskin, J.; Nizkorodov, S. A., Chemistry of Atmospheric Brown Carbon. *Chem.*
504 *Rev.* **2015**, *115*, 4335-4382. doi:10.1021/cr5006167
- 505 13. Shamjad, P. M.; Tripathi, S. N.; Pathak, R.; Hallquist, M.; Arola, A.; Bergin, M. H.,
506 Contribution of Brown Carbon to Direct Radiative Forcing over the Indo-Gangetic Plain.
507 *Environ Sci Technol* **2015**, *49*, (17), 10474-10481. doi:10.1021/acs.est.5b03368
- 508 14. Chakrabarty, R. K.; Gyawali, M.; Yatavelli, R. L. N.; Pandey, A.; Watts, A. C.; Knue, J.; Chen,
509 L. W. A.; Pattison, R. R.; Tsigart, A.; Samburova, V.; Moosmüller, H., Brown carbon aerosols
510 from burning of boreal peatlands: microphysical properties, emission factors, and implications
511 for direct radiative forcing. *Atmos. Chem. Phys.* **2016**, *16*, (5), 3033-3040. doi:10.5194/acp-
512 16-3033-2016

- 513 15. Zhang, Y.; Forrister, H.; Liu, J.; Dibb, J.; Anderson, B.; Schwarz, J. P.; Perring, A. E.; Jimenez,
514 J. L.; Campuzano-Jost, P.; Wang, Y.; Nenes, A.; Weber, R. J., Top-of-atmosphere radiative
515 forcing affected by brown carbon in the upper troposphere. *Nature Geosci.* **2017**, *10*, 486-489.
516 doi:10.1038/ngeo2960
- 517 16. Brown, H.; Liu, X.; Feng, Y.; Jiang, Y.; Wu, M.; Lu, Z.; Wu, C.; Murphy, S.; Pokhrel, R.,
518 Radiative effect and climate impacts of brown carbon with the Community Atmosphere Model
519 (CAM5). *Atmos. Chem. Phys.* **2018**, *18*, (24), 17745-17768. doi:10.5194/acp-18-17745-2018
- 520 17. Zhang, A.; Wang, Y.; Zhang, Y.; Weber, R. J.; Song, Y.; Ke, Z.; Zou, Y., Modeling global
521 radiative effect of brown carbon: A larger heating source in the tropical free troposphere than
522 black carbon. *Atmos. Chem. Phys. Discuss.* **2019**, *2019*, 1-36. doi:10.5194/acp-2019-594
- 523 18. Tuccella, P.; Curci, G.; Pitari, G.; Lee, S.; Jo, D. S., Direct radiative effect of absorbing
524 aerosols: sensitivity to mixing state, brown carbon and soil dust refractive index and shape.
525 *Journal of Geophysical Research: Atmospheres* **2020**, *125*, (2), e2019JD030967.
526 doi:10.1029/2019JD030967
- 527 19. Mukai, H.; Ambe, Y., Characterization of a humic acid-like brown substance in airborne
528 particulate matter and tentative identification of its origin. *Atmospheric Environment (1967)*
529 **1986**, *20*, (5), 813-819. doi:[https://doi.org/10.1016/0004-6981\(86\)90265-9](https://doi.org/10.1016/0004-6981(86)90265-9)
- 530 20. Hecobian, A.; Zhang, X.; Zheng, M.; Frank, N.; Edgerton, E. S.; Weber, R. J., Water-soluble
531 organic aerosol material and the light-absorption characteristics of aqueous extracts measured
532 over the southeastern United States. *Atmos. Chem. Phys.* **2010**, *10*, 5965-5977.
533 doi:10.5194/acp-10-5965-2010
- 534 21. Nozriere, B.; Dziedzic, P.; Cordova, A., Formation of secondary light-absorbing "fulvic-like"
535 oligomers: a common process in aqueous and ionic atmospheric particles? *Geophys. Res. Lett.*
536 **2007**, *34*, L21812. doi:10.1029/2007GL031300
- 537 22. Galloway, M. M.; Chhabra, P. S.; Chan, A. W. H.; Surratt, J. D.; Flagan, R. C.; Seinfeld, J. H.;
538 Keutsch, F. N., Glyoxal uptake on ammonium sulphate seed aerosol: reaction products and
539 reversibility of uptake under dark and irradiated conditions. *Atmos. Chem. Phys.* **2009**, *9*, 3331-
540 3345. doi:10.5194/acp-9-3331-2009
- 541 23. Shapiro, E. L.; Szprengiel, J.; Sareen, N.; Jen, C. N.; Giordano, M. R.; McNeill, V. F., Light-
542 absorbing secondary organic material formed by glyoxal in aqueous aerosol mimics. *Atmos.*
543 *Chem. Phys.* **2009**, *9*, 2289-2300. doi:10.5194/acp-9-2289-2009
- 544 24. Yasmeen, F.; Sauret, N.; Gal, J. F.; Maria, P. C.; Massi, L.; Maenhaut, W.; Claeys, M.,
545 Characterization of oligomers from methylglyoxal under dark conditions: a pathway to
546 produce secondary organic aerosol through cloud processing during nighttime. *Atmos. Chem.*
547 *Phys.* **2010**, *10*, (8), 3803-3812. doi:10.5194/acp-10-3803-2010
- 548 25. Sareen, N.; Schwier, A. N.; Shapiro, E. L.; Mitroo, D.; McNeill, V. F., Secondary organic
549 material formed by methylglyoxal in aqueous aerosol mimics. *Atmos. Chem. Phys.* **2010**, *10*,
550 997-1016. doi:10.5194/acp-10-997-2010
- 551 26. Hawkins, L. N.; Lemire, A. N.; Galloway, M. M.; Corrigan, A. L.; Turley, J. J.; Espelien, B.
552 M.; De Haan, D. O., Maillard Chemistry in Clouds and Aqueous Aerosol As a Source of
553 Atmospheric Humic-Like Substances. *Environ Sci Technol* **2016**, *50*, 7443-7452.
554 doi:10.1021/acs.est.6b00909
- 555 27. Gao, Y.; Zhang, Y., Formation and photochemical investigation of brown carbon by
556 hydroxyacetone reactions with glycine and ammonium sulfate. *RSC Adv.* **2018**, *8*, (37), 20719-
557 20725. doi:10.1039/C8RA02019A

- 558 28. Noziere, B.; Cordova, A., A kinetic and mechanistic study of the amino acid catalyzed aldol
559 condensation of acetaldehyde in aqueous and salt solutions. *J. Phys. Chem.* **2008**, *112*, (13),
560 2827-2837. doi:10.1021/jp7096845
- 561 29. Altieri, K. E.; Seitzinger, S. P.; Carlton, A. G.; Turpin, B. J.; Klein, G. C.; Marshall, A. G.,
562 Oligomers formed through in-cloud methylglyoxal reactions: chemical composition,
563 properties, and mechanisms investigated by ultra-high resolution FT-ICR mass spectrometry.
564 *Atmos. Environ.* **2008**, *42*, 1476-1490. doi:10.1016/j.atmosenv.2007.11.015
- 565 30. Kampf, C. J.; Jakob, R.; Hoffmann, T., Identification and characterization of aging products in
566 the glyoxal/ammonium sulfate system -- implications for light-absorbing material in
567 atmospheric aerosols. *Atmos. Chem. Phys.* **2012**, *12*, 6323-6333. doi:10.5194/acp-12-6323-
568 2012
- 569 31. Lin, P.; Laskin, J.; Nizkorodov, S. A.; Laskin, A., Revealing Brown Carbon Chromophores
570 Produced in Reactions of Methylglyoxal with Ammonium Sulfate. *Environ Sci Technol* **2015**,
571 *49*, (24), 14257-14266. doi:10.1021/acs.est.5b03608
- 572 32. De Haan, D. O.; Hawkins, L. N.; Welsh, H. G.; Pednekar, R.; Casar, J. R.; Pennington, E. A.;
573 de Loera, A.; Jimenez, N. G.; Symons, M. A.; Zauscher, M.; Pajunoja, A.; Caponi, L.;
574 Cazaunau, M.; Formenti, P.; Gratien, A.; Pangui, E.; Doussin, J. F., Brown carbon production
575 in ammonium- or amine-containing aerosol particles by reactive uptake of methylglyoxal and
576 photolytic cloud cycling. *Environmental Science & Technology* **2017**, *in press*.
577 doi:10.1021/acs.est.7b00159
- 578 33. Hawkins, L. N.; Welsh, H. G.; Alexander, M. V., Evidence for pyrazine-based chromophores
579 in cloud water mimics containing methylglyoxal and ammonium sulfate. *Atmos. Chem. Phys.*
580 **2018**, *18*, (16), 12413-12431. doi:10.5194/acp-18-12413-2018
- 581 34. Chang, J. L.; Thompson, J. E., Characterization of colored products formed during irradiation
582 of solutions containing H₂O₂ and phenolic compounds. *Atmos. Environ.* **2010**, *44*, 541-551.
583 doi:10.1016/j.atmosenv.2009.10.042
- 584 35. Ofner, J.; Krüger, H. U.; Grothe, H.; Schmitt-Kopplin, P.; Whitmore, K.; Zetzsch, C., Physico-
585 chemical characterization of SOA derived from catechol and guaiacol - a model substance for
586 the aromatic fraction of atmospheric HULIS. *Atmos. Chem. Phys.* **2011**, *11*, (1), 1-15.
587 doi:10.5194/acp-11-1-2011
- 588 36. Yu, L.; Smith, J.; Laskin, A.; Anastasio, C.; Laskin, J.; Zhang, Q., Chemical characterization
589 of SOA formed from aqueous-phase reactions of phenols with the triplet excited state of
590 carbonyl and hydroxyl radical. *Atmos. Chem. Phys.* **2014**, *14*, (24), 13801-13816, 16 pp.
591 doi:10.5194/acp-14-13801-2014
- 592 37. Yu, L.; Smith, J.; Laskin, A.; George, K. M.; Anastasio, C.; Laskin, J.; Dillner, A. M.; Zhang,
593 Q., Molecular transformations of phenolic SOA during photochemical aging in the aqueous
594 phase: competition among oligomerization, functionalization, and fragmentation. *Atmos.*
595 *Chem. Phys.* **2016**, *16*, (7), 4511-4527. doi:10.5194/acp-16-4511-2016
- 596 38. Smith, J. D.; Kinney, H.; Anastasio, C., Phenolic carbonyls undergo rapid aqueous
597 photodegradation to form low-volatility, light-absorbing products. *Atmos. Environ.* **2016**, *126*,
598 36-44. doi:<http://dx.doi.org/10.1016/j.atmosenv.2015.11.035>
- 599 39. Xu, J.; Cui, T.; Fowler, B.; Fankhauser, A.; Yang, K.; Surratt, J. D.; McNeill, V. F., Aerosol
600 Brown Carbon from Dark Reactions of Syringol in Aqueous Aerosol Mimics. *ACS Earth and*
601 *Space Chemistry* **2018**, *2*, (6), 608-617. doi:10.1021/acsearthspacechem.8b00010
- 602 40. Vione, D.; Albinet, A.; Barsotti, F.; Mekic, M.; Jiang, B.; Minero, C.; Brigante, M.;
603 Gligorovski, S., Formation of substances with humic-like fluorescence properties, upon

- 604 photoinduced oligomerization of typical phenolic compounds emitted by biomass burning.
605 *Atmos. Environ.* **2019**, *206*, 197-207. doi:<https://doi.org/10.1016/j.atmosenv.2019.03.005>
- 606 41. Lavi, A.; Lin, P.; Bhaduri, B.; Carmieli, R.; Laskin, A.; Rudich, Y., Characterization of Light-
607 Absorbing Oligomers from Reactions of Phenolic Compounds and Fe(III). *ACS Earth and*
608 *Space Chemistry* **2017**. doi:10.1021/acsearthspacechem.7b00099
- 609 42. Al Nimer, A.; Rocha, L.; Rahman, M. A.; Nizkorodov, S. A.; Al-Abadleh, H. A., Effect of
610 Oxalate and Sulfate on Iron-Catalyzed Secondary Brown Carbon Formation. *Environ Sci*
611 *Technol* **2019**, *53*, (12), 6708-6717. doi:10.1021/acs.est.9b00237
- 612 43. Link, N.; Removski, N.; Yun, J.; Fleming, L. T.; Nizkorodov, S. A.; Bertram, A. K.; Al-
613 Abadleh, H. A., Dust-Catalyzed Oxidative Polymerization of Catechol and Its Impacts on Ice
614 Nucleation Efficiency and Optical Properties. *ACS Earth and Space Chemistry* **2020**.
615 doi:10.1021/acsearthspacechem.0c00107
- 616 44. De Haan, D. O.; Hawkins, L. N.; Tolbert, M. A.; Doussin, J. F., Glyoxal's impact on dry
617 ammonium salts: fast and reversible surface aerosol browning (Raw Data). *Chemistry and*
618 *Biochemistry: Faculty Scholarship (Digital Repository)* **2020**, (40).
619 doi:<https://doi.org/10.22371/02.2020.006>
- 620 45. Lee, H. J.; Aiona, P. K.; Laskin, A.; Laskin, J.; Nizkorodov, S. A., Effect of solar radiation on
621 the optical properties and molecular composition of laboratory proxies of atmospheric brown
622 carbon. *Environ. Sci. Technol.* **2014**, *48*, (17), 10217-10226. doi:10.1021/es502515r
- 623 46. Dasari, S.; Andersson, A.; Bikkina, S.; Holmstrand, H.; Budhavant, K.; Satheesh, S.; Asmi, E.;
624 Kesti, J.; Backman, J.; Salam, A.; Bisht, D. S.; Tiwari, S.; Hameed, Z.; Gustafsson, Ö.,
625 Photochemical degradation affects the light absorption of water-soluble brown carbon in the
626 South Asian outflow. *Science Advances* **2019**, *5*, (1), eaau8066. doi:10.1126/sciadv.aau8066
- 627 47. O'Brien, R. E.; Kroll, J. H., Photolytic Aging of Secondary Organic Aerosol: Evidence for a
628 Substantial Photo-Recalcitrant Fraction. *The Journal of Physical Chemistry Letters* **2019**, *10*,
629 (14), 4003-4009. doi:10.1021/acs.jpcclett.9b01417
- 630 48. Browne, E. C.; Zhang, X.; Franklin, J. P.; Ridley, K. J.; Kirchstetter, T. W.; Wilson, K. R.;
631 Cappa, C. D.; Kroll, J. H., Effect of heterogeneous oxidative aging on light absorption by
632 biomass-burning organic aerosol. *Aerosol Sci. Technol.* **2019**, 1-15.
633 doi:10.1080/02786826.2019.1599321
- 634 49. Fleming, L. T.; Lin, P.; Roberts, J. M.; Selimovic, V.; Yokelson, R.; Laskin, J.; Laskin, A.;
635 Nizkorodov, S. A., Molecular composition and photochemical lifetimes of brown carbon
636 chromophores in biomass burning organic aerosol. *Atmos. Chem. Phys.* **2020**, *20*, (2), 1105-
637 1129. doi:10.5194/acp-20-1105-2020
- 638 50. Jones, S. H.; Friederich, P.; Donaldson, D. J., Photochemical Aging of Levitated Aqueous
639 Brown Carbon Droplets. *ACS Earth and Space Chemistry* **2021**.
640 doi:10.1021/acsearthspacechem.1c00005
- 641 51. Chen, L.-W. A.; Chow, J. C.; Wang, X.; Cao, J.; Mao, J.; Watson, J. G., Brownness of Organic
642 Aerosol over the United States: Evidence for Seasonal Biomass Burning and Photobleaching
643 Effects. *Environ Sci Technol* **2021**. doi:10.1021/acs.est.0c08706
- 644 52. Rossignol, S.; Aregahegn, K. Z.; Tinel, L.; Fine, L.; Noziere, B.; George, C., Glyoxal Induced
645 Atmospheric Photosensitized Chemistry Leading to Organic Aerosol Growth. *Environ. Sci.*
646 *Technol.* **2014**, *48*, (6), 3218-3227. doi:10.1021/es405581g
- 647 53. Chen, Q.; Mu, Z.; Xu, L.; Wang, M.; Wang, J.; Shan, M.; Fan, X.; Song, J.; Wang, Y.; Lin, P.;
648 Du, L., Triplet-state organic matter in atmospheric aerosols: Formation characteristics and

- 649 potential effects on aerosol aging. *Atmos. Environ.* **2021**, *252*, 118343.
650 doi:<https://doi.org/10.1016/j.atmosenv.2021.118343>
- 651 54. Jiang, W.; Misovich, M. V.; Hettiyadura, A. P. S.; Laskin, A.; McFall, A. S.; Anastasio, C.;
652 Zhang, Q., Photosensitized Reactions of a Phenolic Carbonyl from Wood Combustion in the
653 Aqueous Phase—Chemical Evolution and Light Absorption Properties of AqSOA. *Environ*
654 *Sci Technol* **2021**. doi:10.1021/acs.est.0c07581
- 655 55. Zhao, R.; Lee, A. K. Y.; Abbatt, J. P. D., Investigation of Aqueous-Phase Photooxidation of
656 Glyoxal and Methylglyoxal by Aerosol Chemical Ionization Mass Spectrometry: Observation
657 of Hydroxyhydroperoxide Formation. *The Journal of Physical Chemistry A* **2012**, *116*, (24),
658 6253-6263. doi:10.1021/jp211528d
- 659 56. Sareen, N.; Moussa, S. G.; McNeill, V. F., Photochemical Aging of Light-Absorbing
660 Secondary Organic Aerosol Material. *The Journal of Physical Chemistry A* **2013**, *117*, (14),
661 2987-2996. doi:10.1021/jp309413j
- 662 57. Zhao, R.; Lee, A. K. Y.; Huang, L.; Li, X.; Yang, F.; Abbatt, J. P. D., Photochemical processing
663 of aqueous atmospheric brown carbon. *Atmos. Chem. Phys.* **2015**, *15*, (11), 6087-6100.
664 doi:10.5194/acp-15-6087-2015
- 665 58. Aiona, P. K.; Lee, H. J.; Leslie, R.; Lin, P.; Laskin, A.; Laskin, J.; Nizkorodov, S. A.,
666 Photochemistry of Products of the Aqueous Reaction of Methylglyoxal with Ammonium
667 Sulfate. *ACS Earth and Space Chemistry* **2017**, *1*, (8), 522-532.
668 doi:10.1021/acsearthspacechem.7b00075
- 669 59. Vo, L.; Legaard, E.; Thrasher, C.; Jaffe, A.; Berden, G.; Martens, J.; Oomens, J.; O'Brien, R.
670 E., UV/Vis and IRMPD Spectroscopic Analysis of the Absorption Properties of Methylglyoxal
671 Brown Carbon. *ACS Earth and Space Chemistry* **2021**, *5*, (4), 910-919.
672 doi:10.1021/acsearthspacechem.1c00022
- 673 60. Wong, J. P. S.; Nenes, A.; Weber, R. J., Changes in Light Absorptivity of Molecular Weight
674 Separated Brown Carbon Due to Photolytic Aging. *Environ Sci Technol* **2017**, *51*, (15), 8414-
675 8421. doi:10.1021/acs.est.7b01739
- 676 61. He, Q.; Tomaz, S.; Li, C.; Zhu, M.; Meidan, D.; Riva, M.; Laskin, A.; Brown, S. S.; George,
677 C.; Wang, X.; Rudich, Y., Optical Properties of Secondary Organic Aerosol Produced by
678 Nitrate Radical Oxidation of Biogenic Volatile Organic Compounds. *Environ Sci Technol*
679 **2021**. doi:10.1021/acs.est.0c06838
- 680 62. Wang, J.; Doussin, J. F.; Perrier, S.; Perraudin, E.; Katrib, Y.; Pangui, E.; Picquet-Varrault, B.,
681 Design of a new multi-phase experimental simulation chamber for atmospheric photosmog,
682 aerosol and cloud chemistry research. *Atmos. Meas. Tech.* **2011**, *4*, 2465-2494.
683 doi:10.5194/amt-4-2465-2011
- 684 63. De Haan, D. O.; Tapavicza, E.; Riva, M.; Cui, T.; Surratt, J.; Smith, A. C.; Jordan, M.-C.;
685 Nilakantan, S.; Almodovar, M.; Stewart, T. N.; de Loera, A.; De Haan, A. C.; Cazaunau, M.;
686 Gratien, A.; Pangui, E.; Doussin, J. F., Nitrogen-containing, light-absorbing oligomers
687 produced in aerosol particles exposed to methylglyoxal, photolysis, and cloud cycling.
688 *Environ. Sci. Technol.* **2018**, *52*, (7), 4061-4071. doi:10.1021/acs.est.7b06105
- 689 64. Lin, P.; Fleming, L. T.; Nizkorodov, S. A.; Laskin, J.; Laskin, A., Comprehensive Molecular
690 Characterization of Atmospheric Brown Carbon by High Resolution Mass Spectrometry with
691 Electrospray and Atmospheric Pressure Photoionization. *Anal. Chem.* **2018**, *90*, (21), 12493-
692 12502. doi:10.1021/acs.analchem.8b02177

- 693 65. Powelson, M. H.; Espelien, B. M.; Hawkins, L. N.; Galloway, M. M.; De Haan, D. O., Brown
694 carbon formation by aqueous-phase aldehyde reactions with amines and ammonium sulfate.
695 *Environ Sci Technol* **2014**, *48*, (2), 985-993. doi:10.1021/es4038325
- 696 66. Trainic, M.; Riziq, A. A.; Lavi, A.; Rudich, Y., Role of interfacial water in the heterogeneous
697 uptake of glyoxal by mixed glycine and ammonium sulfate aerosols. *Journal of Physical*
698 *Chemistry A* **2012**, *116*, 5948-5957. doi:10.1021/jp2104837
- 699 67. Drozd, G. T.; McNeill, V. F., Organic matrix effects on the formation of light-absorbing
700 compounds from [small alpha]-dicarbonyls in aqueous salt solution. *Environmental Science:*
701 *Processes & Impacts* **2014**, *16*, (4), 741-747. doi:10.1039/C3EM00579H
- 702 68. Gómez Alvarez, E.; Wortham, H.; Strekowski, R.; Zetzsch, C.; Gligorovski, S., Atmospheric
703 Photosensitized Heterogeneous and Multiphase Reactions: From Outdoors to Indoors. *Environ*
704 *Sci Technol* **2012**, *46*, (4), 1955-1963. doi:10.1021/es2019675
- 705 69. Saleh, R., From Measurements to Models: Toward Accurate Representation of Brown Carbon
706 in Climate Calculations. *Current Pollution Reports* **2020**, *6*, (2), 90-104. doi:10.1007/s40726-
707 020-00139-3
- 708 70. Pospisilova, V.; Bell, D. M.; Lamkaddam, H.; Bertrand, A.; Wang, L.; Bhattu, D.; Zhou, X.;
709 Dommen, J.; Prevot, A. S. H.; Baltensperger, U.; El Haddad, I.; Slowik, J. G.,
710 Photodegradation of α -Pinene Secondary Organic Aerosol Dominated by Moderately Oxidized
711 Molecules. *Environ Sci Technol* **2021**. doi:10.1021/acs.est.0c06752
- 712 71. Klodt, A. L.; Zhang, K.; Olsen, M. W.; Fernandez, J. L.; Furche, F.; Nizkorodov, S. A., Effect
713 of Ammonium Salts on the Decarboxylation of Oxaloacetic Acid in Atmospheric Particles.
714 *ACS Earth and Space Chemistry* **2021**, *5*, (4), 931-940.
715 doi:10.1021/acsearthspacechem.1c00025
- 716 72. Axson, J. L.; Takahashi, K.; De Haan, D. O.; Vaida, V., Gas-phase water-mediated equilibrium
717 between methylglyoxal and its geminal diol. *P. Natl. Acad. Sci. USA* **2010**, *107*, (15), 6687-
718 6692. doi:10.1073/pnas.0912121107
- 719 73. Kroll, J. A.; Hansen, A. S.; Møller, K. H.; Axson, J. L.; Kjaergaard, H. G.; Vaida, V.,
720 Ultraviolet Spectroscopy of the Gas Phase Hydration of Methylglyoxal. *ACS Earth and Space*
721 *Chemistry* **2017**, *1*, (6), 345-352. doi:10.1021/acsearthspacechem.7b00054
- 722 74. Grace, D. N.; Sharp, J. R.; Holappa, R. E.; Lugos, E. N.; Sebold, M. B.; Griffith, D. R.;
723 Hendrickson, H. P.; Galloway, M. M., Heterocyclic Product Formation in Aqueous Brown
724 Carbon Systems. *ACS Earth and Space Chemistry* **2019**, *3*, (11), 2472-2481.
725 doi:10.1021/acsearthspacechem.9b00235
- 726 75. Aregahegn, K. Z.; Noziere, B.; George, C., Organic aerosol formation photo-enhanced by the
727 formation of secondary photosensitizers in aerosols. *Faraday Discuss.* **2013**, *165*, 123-134.
728 doi:10.1039/c3fd00044c
- 729 76. Teich, M.; van Pinxteren, D.; Kecorius, S.; Wang, Z.; Herrmann, H., First quantification of
730 imidazoles in ambient aerosol particles: Potential photosensitizers, brown carbon constituents,
731 and hazardous components. *Environ Sci Technol* **2016**, *50*, 1166-1173.
732 doi:10.1021/acs.est.5b05474
- 733 77. Zhu, Y.; Xiao, L.; Zhao, M.; Zhou, J.; Zhang, Q.; Wang, H.; Li, S.; Zhou, H.; Wu, J.; Tian, Y.,
734 A Series of Imidazole Derivatives: Synthesis, Two-Photon Absorption, and Application for
735 Bioimaging. *BioMed Research International* **2015**, *2015*, 965386. doi:10.1155/2015/965386
- 736 78. Frka, S.; Dautović, J.; Kozarac, Z.; Ćosović, B.; Hoffer, A.; Kiss, G., Surface-active substances
737 in atmospheric aerosol: an electrochemical approach. *Tellus B: Chemical and Physical*
738 *Meteorology* **2012**, *64*, (1), 18490. doi:10.3402/tellusb.v64i0.18490

- 739 79. Tan, Y.; Lim, Y. B.; Altieri, K. E.; Seitzinger, S. P.; Turpin, B. J., Mechanisms leading to
740 oligomers and SOA through aqueous photooxidation: insights from OH radical oxidation of
741 acetic acid and methylglyoxal. *Atmos. Chem. Phys.* **2012**, *12*, 801-813. doi:10.5194/acp-12-
742 801-2012
- 743 80. Tan, Y.; Perri, M. J.; Seitzinger, S. P.; Turpin, B. J., Effects of precursor concentration and
744 acidic sulfate in aqueous glyoxal - OH radical oxidation and implications for secondary organic
745 aerosol. *Environ. Sci. Technol.* **2009**, *43*, (21), 8105-8112. doi:10.1021/es901742f
- 746